

PNPLA3 mediates hepatocyte triacylglycerol remodeling[§]

Hanna Ruhanen,^{*,†} Julia Perttilä,^{*} Maarit Hölttä-Vuori,^{*,§} You Zhou,^{*} Hannele Yki-Järvinen,^{*,**} Elina Ikonen,^{*,§} Reijo Käkelä,[†] and Vesa M. Olkkonen^{1,*,§}

Minerva Foundation Institute for Medical Research,^{*} Biomedicum 2U, FI-00290 Helsinki, Finland; and Departments of Biosciences[†] and Medicine,^{**} and Institute of Biomedicine, Anatomy,[§] University of Helsinki, FI-00014 Helsinki, Finland

Abstract The I148M substitution in patatin-like phospholipase domain containing 3 (PNPLA3^{I148M}) determines a genetic form of nonalcoholic fatty liver disease. To elucidate the mode of PNPLA3 action in human hepatocytes, we studied effects of WT PNPLA3 (PNPLA3^{WT}) and PNPLA3^{I148M} on HuH7 cell lipidome after [¹³C]glycerol labeling, cellular turnover of oleic acid labeled with 17 deuterium atoms ([D17] oleic acid) in triacylglycerols (TAGs), and subcellular distribution of the protein variants. PNPLA3^{I148M} induced a net accumulation of unlabeled TAGs, but not newly synthesized total [¹³C]TAGs. Principal component analysis (PCA) revealed that both PNPLA3^{WT} and PNPLA3^{I148M} induced a relative enrichment of TAGs with saturated FAs or MUFAs, with concurrent enrichment of polyunsaturated phosphatidylcholines. PNPLA3^{WT} associated in PCA with newly synthesized [¹³C]TAGs, particularly 52:1 and 50:1, while PNPLA3^{I148M} associated with similar preexisting TAGs. PNPLA3^{WT} overexpression resulted in increased [D17]oleic acid labeling of TAGs during 24 h, and after longer incubations their turnover was accelerated, effects not detected with PNPLA3^{I148M}. PNPLA3^{I148M} localized more extensively to lipid droplets (LDs) than PNPLA3^{WT}, suggesting that the substitution alters distribution of PNPLA3 between LDs and endoplasmic reticulum/cytosol. This study reveals a function of PNPLA3 in FA-selective TAG remodeling, resulting in increased TAG saturation. A defect in TAG remodeling activity likely contributes to the TAG accumulation observed in cells expressing PNPLA3^{I148M}.—Ruhanen, H., J. Perttilä, M. Hölttä-Vuori, Y. Zhou, H. Yki-Järvinen, E. Ikonen, R. Käkelä, and V. M. Olkkonen. PNPLA3 mediates hepatocyte triacylglycerol remodeling. *J. Lipid Res.* 2014. 55: 739–746.

Supplementary key words adiponutrin • lipase • lipid droplet • lipidomics • nonalcoholic fatty liver disease • patatin-like phospholipase domain containing 3

Nonalcoholic fatty liver disease (NAFLD) is a burgeoning health problem closely associated with all features of the metabolic syndrome (1–3) Romeo et al. (4) first described

This study was supported by the Academy of Finland (grant 138114 to J.P. and grant 218066 to E.I.), the Finnish government EVO funds (H.Y.-J.), the Sigrid Juselius Foundation, the Liv och Hälsa Foundation (V.M.O., H.Y.-J.), and the Magnus Ehrnrooth Foundation (V.M.O.).

Manuscript received 22 December 2013 and in revised form 6 February 2014.

Published, JLR Papers in Press, February 7, 2014
DOI 10.1194/jlr.M046607

Copyright © 2014 by the American Society for Biochemistry and Molecular Biology, Inc.

This article is available online at <http://www.jlr.org>

a single-nucleotide polymorphism (rs738409; C>G/I148M) in the patatin-like phospholipase domain containing 3 (PNPLA3, adiponutrin) gene, to be strongly associated with NAFLD. A meta-analysis of 16 studies demonstrated that homozygous carriers of PNPLA3^{I148M} have on the average a 73% higher liver fat content than weight-matched homozygous carriers of the major allele (5). However, NAFLD associated with PNPLA3^{I148M} is distinct from obesity-associated common NAFLD, as it is not characterized by features of the metabolic syndrome such as hyperinsulinemia or dyslipidemia (1, 5).

In vitro assays using recombinant PNPLA3 have suggested that the WT PNPLA3 (PNPLA3^{WT}) hydrolyzes emulsified triacylglycerol (TAG) and that the I148M substitution in PNPLA3 (PNPLA3^{I148M}) abolishes this activity (6–8). Moreover, the protein was shown to display a transacylase activity (7), and to prefer oleic acid (18:1n-9) as the fatty acyl moiety (9). Opposing a putative role as a lipase, PNPLA3 is induced by glucose and insulin (10–12) and is a target gene of the lipogenic transcription factors SREBP-1c and the carbohydrate responsive element binding protein, ChREBP (13–16). Kumari et al. (17) suggested that the protein acts as lipogenic lysophosphatidic acid (LPA) acyltransferase, converting LPA to phosphatidic acid (PA), and that the I148M substitution increases this activity. Because PA acts as a precursor for both phospholipids and TAGs, this provided an alternative explanation for the hepatic fat accumulation in the PNPLA3^{I148M} allele carriers. Even though PNPLA3 knockout mice have no metabolic phenotype (18, 19), Kumashiro et al. (20) reported that reducing PNPLA3 in rat liver via RNA interference prevented hepatic steatosis, an effect attributed to

Abbreviations: D17, labeled with 17 deuterium atoms; DAG, diacylglycerol; ER, endoplasmic reticulum; GFP, green fluorescent protein; LD, lipid droplet; LPA, lysophosphatidic acid; NAFLD, nonalcoholic fatty liver disease; PA, phosphatidic acid; PC, phosphatidylcholine; PC2, principal component 2; PCA, principal component analysis; PNPLA3, patatin-like phospholipase domain containing 3; SFA, saturated FA; SIMCA, soft independent modeling of class analogy; TAG, triacylglycerol.

¹To whom correspondence should be addressed.

e-mail: vesa.olkkonen@helsinki.fi

[§]The online version of this article (available at <http://www.jlr.org>) contains supplementary data in the form of five tables.

decreased FA esterification. In apparent contradiction with these findings, the study by Pirazzi et al. (21) in human subjects showed a reduced rate of large TAG-rich VLDL secretion in I148M carriers versus 148II homozygotes for any amount of liver fat, suggesting that PNPLA3^{I148M} represents a loss-of-function mutant that promotes hepatocyte TAG accumulation via reduction of VLDL assembly, putatively by inhibiting the mobilization of TAG FAs. Li et al. (22) recently developed transgenic mice overexpressing WT human PNPLA3 or the I148M variant either in liver or adipose tissue. Expression of PNPLA3^{I148M}, but not the WT protein, in the liver recapitulated the fatty liver phenotype. The above-mentioned metabolic studies suggested that the increase in hepatic TAGs associated with the I148M allele results from multiple changes in hepatic TAG metabolism. Both PNPLA3^{WT} and PNPLA3^{I148M} localize prominently on cytoplasmic lipid droplets (LDs) (6, 23). Thus, the mechanism by which PNPLA3^{I148M} causes NAFLD is still controversial.

In the present study, we examined the mechanisms by which PNPLA3 and its I148M variant modify the lipid content and composition of human hepatic cells *in vitro*. We acutely overexpressed PNPLA3^{WT} or PNPLA3^{I148M} in the HuH7 hepatoma cell line, which expresses no detectable endogenous PNPLA3, cultured the cells under stable isotope labeling of TAGs with [¹³C]glycerol, and performed turnover experiments with oleic acid (18:1n-9) labeled with 17 deuterium atoms ([D17]18:1n-9). Cellular TAGs, diacylglycerols (DAGs), and phospholipids were examined by MS. Further evidence of the functional difference between PNPLA3^{WT} and PNPLA3^{I148M} was obtained by comparing their subcellular distributions in the presence or absence of FA supplementation.

MATERIALS AND METHODS

Cell culture

HuH7 cells (24) were grown in MEM (GIBCO/Life Technologies, Carlsbad, CA), containing 10% FBS, 2 mM L-glutamine, 100 U/ml penicillin, and 100 µg/ml streptomycin.

cDNA constructs and antibodies

The *PNPLA3* cDNA open-reading frame corresponding to NM_025225 was isolated by PCR from human subcutaneous adipose tissue and inserted into the *EcoRI* site of pcDNA4HisMaxC (Invitrogen/Life Technologies) and pEGFP-C2 (Clontech/Takara Bio, Mountain View, CA). The I148M substitution corresponding to the rs738409 G allele was introduced in the *PNPLA3* cDNA with the Quikchange site-directed mutagenesis kit (Stratagene, La Jolla, CA). Rabbit anti-PNPLA3, anti-β-actin (Sigma-Aldrich, St. Louis, MO), and anti-green fluorescent protein (GFP) (Life Technologies, Grand Island, NY) were employed for detection of Western blots.

PNPLA3 overexpression and treatments of cells

For analysis of preexisting and newly synthesized glycerolipids, HuH7 cells cultured on 6-well plates were transfected with an empty vector, *PNPLA3*^{WT}, or *PNPLA3*^{I148M}-pcDNAHisMaxC using Lipofectamine 2000TM (Invitrogen). One day after transfection medium was changed to a labeling medium containing 500 µg/ml of [¹³C]glycerol (Cambridge Isotope Laboratories, Andover, MA), incubated for 24 h, washed with PBS, and scraped into 1 ml of

ice-cold 0.25 M sucrose. An aliquot of 100 µl was withdrawn for total cell protein analysis using the BCA assay (Thermo Fisher Scientific, Waltham, MA). The data for glycerolipid synthesis represents seven parallel cell cultures originating from two independent labeling experiments [the TAG and phosphatidylcholine (PC) species profiles in both experiments were in general the same and are shown in detail for the first experiment, supplementary Tables I, II].

For analysis of TAG hydrolysis, the cells were cultured on 6 cm dishes and transfected as described above, washed, and changed into growth medium supplemented with 5% delipidated FBS and 5 µM triacsin C (Enzo Life Sciences, Farmingdale, NY). After 0, 6, or 24 h chase times in this medium, the cells were washed with PBS and scraped into 1 ml of ice-cold 0.25 M sucrose.

For analysis of TAG turnover, HuH7 cells in complete growth medium without antibiotics were transfected for 24 h as above and then labeled for 24, 48, or 72 h with 15 µg/ml [D17]18:1n-9 (71-1851; Larodan Fine Chemicals, Malmö, Sweden) using fat-free BSA as a vehicle. The lipids were extracted, and the unlabeled and labeled TAG species detected by MS as detailed below.

Lipid extraction, MS, and GC of FAs

Cellular lipids were extracted according to Folch et al. (25) and dissolved in chloroform:methanol 1:2. Immediately before MS, 1% NH₄OH was added along with an internal standard mixture containing polar and neutral lipid species. The samples were infused into an ion trap ESI mass spectrometer (Esquire-LC, Bruker-Franzen Analytik, Bremen, Germany) and spectra recorded by employing both positive and negative ionization mode in the range of *m/z* 500–1,000 (26). The unlabeled [M] and [¹³C]glycerol-labeled [M+3] ions were resolved by comparing the spectra of cell samples with or without labeling, and deconvolution into different peaks was performed by the best profile fitting available in LIMS software (27). In addition, FA composition of total lipids was determined by GC as detailed in Käkälä et al. (28). In order to confirm glycerolipid species structures, the precursor scans for the main acyl chains detected by GC were later recorded in ESI-MS/MS experiments for TAGs (positive mode neutral loss scans for the FAs) and PCs (negative mode precursor scans for the FAs of PC formate adducts) using a triple quadrupole mass spectrometer (Agilent 6490 Triple Quad LC/MS with iFunnel Technology; Agilent Technologies, Santa Clara, CA). The [D17]18:1n-9 incorporation into TAG and the following turnover were studied using the triple quadrupole equipment by scanning for the positive mode neutral loss of the unlabeled and deuterated 18:1n-9 moiety.

For analysis of DAGs and PAs by ion trap ESI-MS, cellular lipids were extracted using a modified Bligh/Dyer procedure (29). First, 800 µl of ice-cold 0.1 N HCl:methanol (1:1) was added to each cell pellet and DAG 24:0 was inserted as an internal standard. Then 400 µl of ice-cold chloroform was added and the separated lower phase was collected, evaporated to dryness under nitrogen flow, and finally the original volume was restored by adding chloroform:methanol (1:9). The mass spectra for the DAG species were recorded in the positive ionization mode over the range of *m/z* 400–750. The spectra for PA species were recorded over the range of *m/z* 600–800 by using samples brought into chloroform:methanol (1:2) and using PA 34:0 as internal standard.

The ion trap ESI-MS spectra were processed by Bruker Daltonics (Billerica, MA) data analysis software and the triple quadrupole ESI-MS/MS spectra by Agilent Mass Hunter software. Individual lipid species were quantified by using the internal standards and the LIMS software (27).

Fluorescence microscopy

To analyze the subcellular distribution of PNPLA3, HuH7 cells were transfected for 48 h with plasmids encoding GFP-PNPLA3^{WT}

or GFP-PNPLA3^{I148M} by using Lipofectamine 2000. Prior to fixation with 4% paraformaldehyde, cells were treated for indicated times with 200 μ M oleic acid-BSA as described (30). For LD visualization, cells were stained immediately after fixation with LipidTox Red (Invitrogen/Life Technologies) according to the manufacturer's instructions and imaged with a TCS SP2 confocal microscope (Leica, Wetzlar, Germany). The percentage of cells exhibiting predominantly reticular/cytosolic PNPLA3 distribution was determined by visual inspection of cells from 10 randomly selected fields under a wide-field AX70 microscope (Olympus, Hamburg, Germany).

Statistical analysis of lipid levels

For univariate comparisons of the cellular lipid levels, statistical significance for the differences between control, PNPLA3^{WT}, and PNPLA3^{I148M} overexpressing samples were assessed by using one-way ANOVA followed by Newman-Keuls test of means (SPSS Statistics, IBM, North Castle, NY). For multivariate comparisons of detailed lipid profiles, principal component analysis (PCA) (Sirius, PRS, Bergen, Norway) was used. The PCA describes compositional differences between the samples, and highlights the lipid species mainly responsible for the variation in the data. PCA was computed using arcsine transformed data and the relative positions of the samples and variables were plotted using the first two principal components. In addition, quantitative multivariate measures of the compositional differences among the sample groups were determined by soft independent modeling of class analogy (SIMCA; Sirius) (31). To analyze the rate of TAG remodeling, regression lines of groups were compared by measuring the effect of a categorical factor on the responding variable, by using the 'aov' function in the 'stats' package of R. The statistical differences in the proportion of cells where PNPLA3 was present in cytosol or endoplasmic reticulum (ER) were tested by Student's *t*-test.

RESULTS

PNPLA3^{I148M} induces net TAG accumulation

We acutely overexpressed PNPLA3^{WT} or PNPLA3^{I148M} in the hepatoma cell line HuH7, which contains no endogenous PNPLA3 protein (with an apparent molecular mass

of 53 kDa) detectable by Western blot analysis (Fig. 1A). After 24 h of transfection, the cells were subjected to 24 h metabolic labeling of glycerolipids with [¹³C]glycerol, and the cellular lipids were thereafter analyzed by MS. After the [¹³C]glycerol labeling (total transfection time of 48 h), the cells expressing PNPLA3^{I148M} displayed a marked net increase of unlabeled TAGs compared with mock-transfected controls, while expression of PNPLA3^{WT} had no such effect (Fig. 1B). While the unlabeled TAGs represent lipids that were present in the cells already before the labeling, the [¹³C]TAGs represent the newly synthesized species. After 48 h of transfection, the concentrations of [¹³C]TAGs were similar in controls and cells expressing either form of PNPLA3 (Fig. 1C), suggesting that PNPLA3 does not primarily enhance de novo TAG synthesis. Consistent with earlier findings (6, 15), when the cells were incubated for 6 or 24 h in a medium supplemented with 5% delipidated serum and the long chain FA-CoA synthase inhibitor Triacsin C, PNPLA3^{I148M} caused a kinetic delay in TAG hydrolysis (data not shown). Thus, PNPLA3^{I148M} expression results in net TAG accumulation in the absence of altered synthesis of TAGs, but with a delay in their hydrolysis.

PNPLA3 induces redistribution of FAs between TAGs and membrane phospholipids

To analyze in detail the effect of PNPLA3 on the hepatocellular glycerolipid dynamics, we studied the lipid species profiles of the [¹³C]glycerol-labeled cells (values for the glycerolipid species from the experiment described in Fig. 2 are listed in supplementary Tables I–IV). According to PCA, the TAG profiles of both PNPLA3^{WT} and PNPLA3^{I148M} cells were found to differ significantly from those of the controls (Fig. 2A). The most important principal component extracted (PC1) explained 35% of the TAG variation between the constructs and reflected the degree of FA unsaturation. Cells expressing either form of PNPLA3 were characterized by increased relative amounts of TAGs with saturated FA (SFA) and MUFA moieties. The WT and I148M cells differed with respect to principal

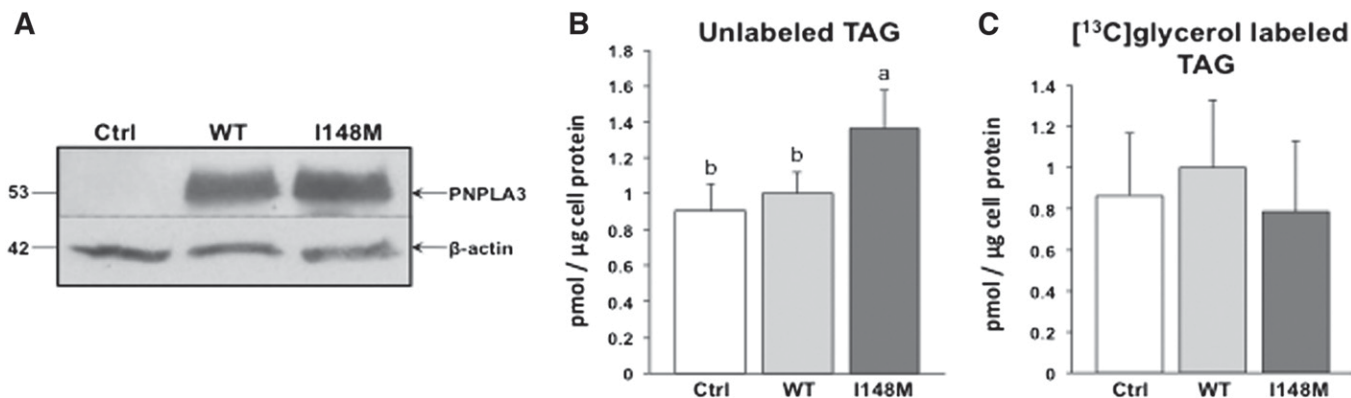


Fig. 1. Overexpression of PNPLA3^{I148M} in HuH7 cells induces net TAG accumulation but does not affect the newly synthesized TAGs. A: Western analysis of mock-transfected controls and cells overexpressing PNPLA3^{WT} or PNPLA3^{I148M}. Beta-actin was probed as a loading control. B: Quantity of total unlabeled TAGs after 24 h of [¹³C]glycerol labeling, analyzed by MS. C: Newly synthesized [¹³C]glycerol-labeled TAGs after 24 h of labeling. The values for panels (B) and (C) originating from separate experiments were normalized by setting the PNPLA3^{WT} average of each experiment to 1. Means with no common letter differ at $P < 0.05$ (one-way ANOVA followed by Newman-Keuls test of means). Error bars, SD; $n = 7$. Ctrl, control.

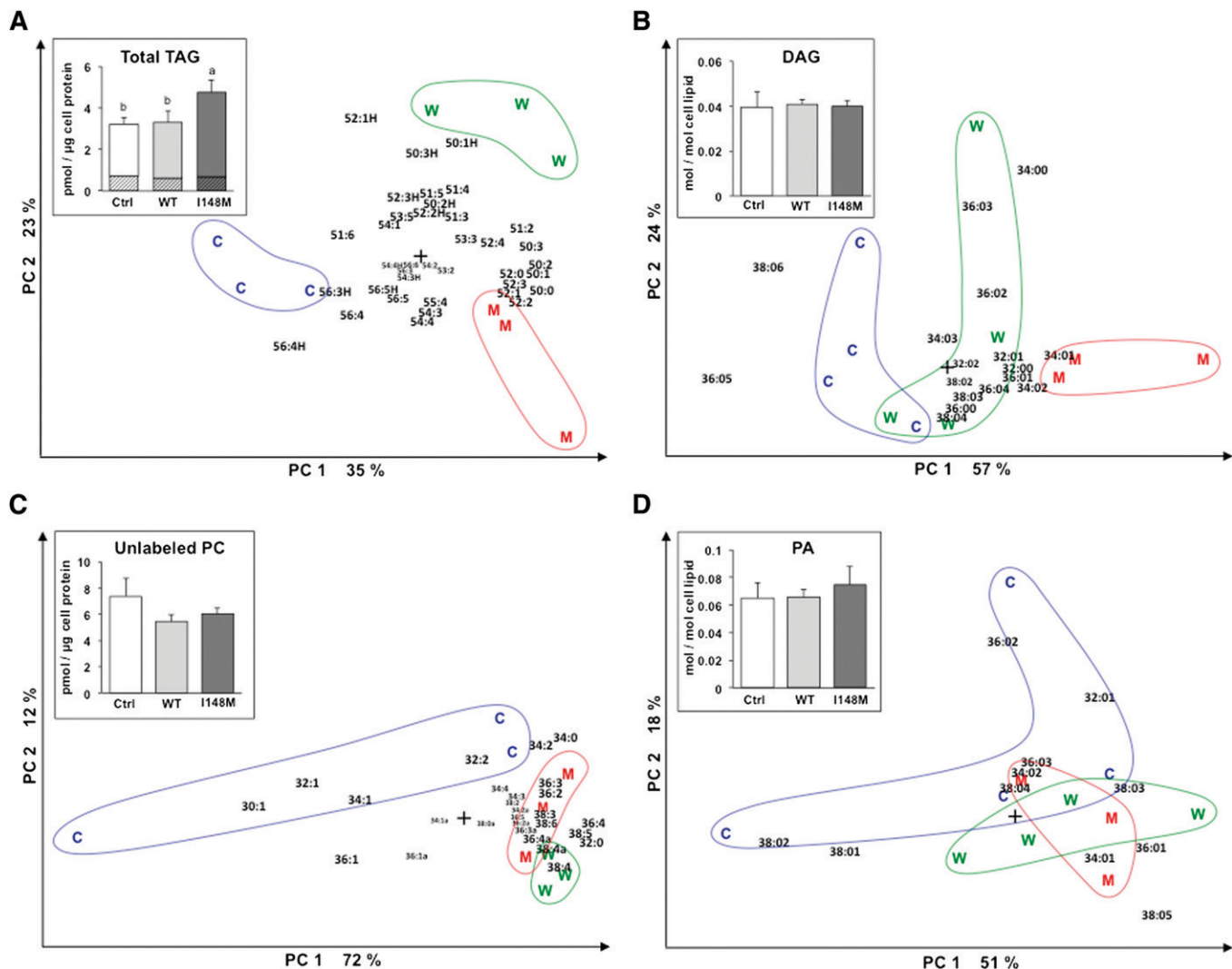


Fig. 2. PCA reveals lipidome differences in HuH7 cells overexpressing PNPLA3^{WT} or PNPLA3^{I148M}. The samples located on the plot farthest from the origin (cross) on one side are relatively enriched in the lipid species farthest on the same side. The larger the distance of any two samples on this plot the more they differ in terms of the whole lipid species profile. A: PCA of TAG species after 24 h of [¹³C]glycerol labeling. Species present in any of the cells at >0.5% were used as variables. Lipid species abbreviations: 56:3H = 56 carbons, 3 double bonds, [¹³C]glycerol labeled, i.e., heavier (H) species; 52:4 = 52 carbons, 4 double bonds, unlabeled. C, control; W, PNPLA3^{WT}; M, PNPLA3^{I148M}. Means with no common letter differ at $P < 0.05$ (one-way ANOVA followed by Newman-Keuls test of means). B: PCA of DAGs. DAG species present at >0.5% were used as variables. C: PCA of PCs. PC species present with >0.5% were used as variables; a = alkyl-acyl species (commonly diacyl species). D: PCA of PAs. PA species present at >1% were used as variables. The total amounts of each lipid class (the major classes, TAG and PC, are displayed in pmol/μg cell protein and the minor classes, DAG and PA, in mol/mol total lipid) are shown as inserts; in (A) the hatched bottom part of the bars indicates the share of [¹³C]-labeled TAGs. The bar graph statistics are as in Fig. 1. Ctrl, control.

component 2 (PC2) (explaining 23% of the variation), a component influenced by the presence/absence of [¹³C]glycerol in certain TAG species. PNPLA3^{WT} cell TAGs (high position on PC2 axis) contained, e.g., more newly synthesized [¹³C]52:1 and [¹³C]50:1 species (52:1H and 50:1H in Fig. 2A) and less of their unlabeled counterparts than the I148M cells (low on PC2 axis). This observation is consistent with a more active remodeling of these TAGs in cells expressing the PNPLA3^{WT} as compared with the PNPLA3^{I148M} cells. The differences between the cells (control, WT, and I148M) seen on the PCA biplot were studied quantitatively by the SIMCA method, which confirmed that the TAG profiles of the three transfected cell pools significantly differed from each other ($P < 0.05$, test graphics

not shown). When applied for DAG species, the PCA followed by SIMCA ($P < 0.05$) showed that the profile of PNPLA3^{I148M}-expressing cells was significantly different from those of the controls and the PNPLA3^{WT} cells: the I148M cells were enriched with species containing SFAs or MUFAs. PNPLA3^{WT} cells localized in the PCA between the PNPLA3^{I148M} and control cells, and did not differ in SIMCA from the latter (Fig. 2B). The total cellular DAG content was unaffected by PNPLA3^{WT}/PNPLA3^{I148M} expression.

Analysis of the species profiles of cellular PCs, the major membrane phospholipid class of mammalian hepatocytes, showed a significant shift (SIMCA, $P < 0.05$) toward species carrying PUFAs in both PNPLA3^{WT}- and PNPLA3^{I148M}-transfected cells, especially arachidonic acid (20:4n-6) (e.g.,

36:4, 38:5, and 38:4), while the total cellular PC content did not differ significantly between the control and PNPLA3^{WT}/PNPLA3^{I148M}-transfected cells (Fig. 2C). Regarding the composition of PC species, cells transfected with either of the PNPLA3 constructs differed significantly (SIMCA, $P < 0.05$) from the controls, and the PNPLA3^{WT} induced a more pronounced shift in the PC species composition than PNPLA3^{I148M} (Fig. 2C). This result, in the face of TAGs enriched with SFAs and MUFAs, suggests net transfer of PUFAs from TAGs to membrane phospholipids by the protein. The same phenomenon was seen in two independent experiments (data of the repeat experiment not shown). In extended cultures beyond 72 h, the FA composition of the PNPLA3^{I148M}-expressing cells was also slightly altered. The relative amounts of MUFAs 18:1n-7 and 16:1n-7 (vacenic and palmitoleic acids, respectively) were significantly increased as compared with the controls or PNPLA3^{WT}-transfected cells (ANOVA, $P < 0.05$; supplementary Table V).

PNPLA3 overexpression has no impact on hepatocellular PAs

Prompted by the report of Kumari et al. (17) suggesting that PNPLA3 displays LPA acyltransferase activity, we analyzed the PA contents and species profiles in the transfected HuH7 cells. The PA patterns of PNPLA3^{WT}/PNPLA3^{I148M}-expressing cells or the total cellular amount of PAs did not differ significantly from the controls (Fig. 2D).

PNPLA3^{WT}, but not PNPLA3^{I148M}, enhances the remodeling of TAGs

To directly assess the possibility that PNPLA3 facilitates the remodeling of hepatocyte TAGs, we carried out labeling of transfected HuH7 cells in serum containing growth medium with stable isotope [D17]18:1n-9, the preferred substrate of PNPLA3 (9), for 24, 48, or 72 h, followed by lipid extraction and mass spectrometric analysis of the TAGs. At the 24 h time point, analysis of the relative amount of [D17]-labeled versus unlabeled 18:1-containing TAGs revealed a significant increase of [D17]18:1n-9 incorporation into TAGs in cells expressing PNPLA3^{WT}, an effect not observed with PNPLA3^{I148M} (Fig. 3). After this time point, the relative amount of [D17] TAGs reduced in PNPLA3^{WT}-expressing cells more rapidly as compared with PNPLA3^{I148M} or the mock-transfected control ($P < 0.01$), all three groups of transfected cells ending up at the same level at the 72 h time point (Fig. 3). These observations suggest that PNPLA3^{WT} enhances both 18:1n-9 incorporation into TAGs and its removal from these lipids, a remodeling activity defective in PNPLA3^{I148M}.

PNPLA3^{I148M} localizes more extensively to LDs than the WT protein

To assess the subcellular distribution and the putative impact of PNPLA3 on LD morphology, we expressed the GFP-tagged WT or I148M proteins in HuH7 cells, followed by LD visualization with the LipidTox Red dye (Fig. 4). In most cells PNPLA3 associated with LDs, but 46% of the cells exhibited, in addition, a more diffuse pattern, most likely reflecting cytosolic and ER distribution. Interestingly, PNPLA3^{I148M} associated more faithfully with LDs, a

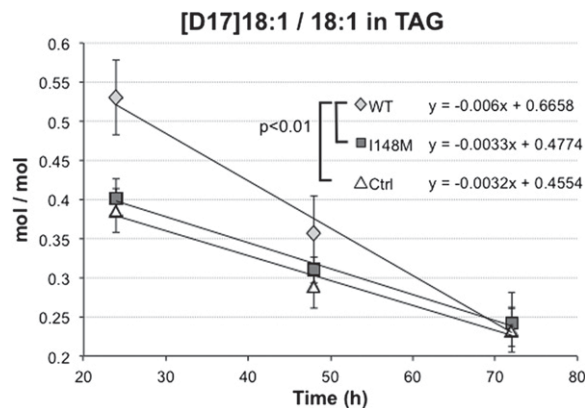


Fig. 3. PNPLA3^{WT}, but not PNPLA3^{I148M}, enhances the hepatocellular remodeling of TAGs. HuH7 cells transfected with empty vector (Ctrl) or the indicated PNPLA3 expression constructs were labeled in complete growth medium with [D17]18:1n-9 as specified in the Materials and Methods, followed by lipid extraction and mass spectrometric quantification of TAG molecular species. The data represent the amount of [D17]18:1n-9-containing TAGs relative to the corresponding unlabeled species, a ratio which decreased rapidly for the PNPLA3^{WT} cells. The data points represent mean \pm SD, $n = 4-5$, and the P value indicates significant difference between the regression models.

diffuse cytosolic/ER distribution being detectable only in 24% of the cells (Fig. 4A, B). Loading of the cells for 24 h with 18:1n-9 to enhance TAG synthesis resulted in an increase of the LD association of both PNPLA3^{WT} and PNPLA3^{I148M} (Fig. 4A, B), suggesting that the lipid content and/or metabolic status of the LDs modulates PNPLA3 association with these organelles. Of note, Western analysis of the cells verified that both the GFP-PNPLA3^{WT} and the GFP-PNPLA3^{I148M} fusion proteins remained intact and were expressed at similar levels (Fig. 4C).

DISCUSSION

The mechanism of PNPLA3 function and the reasons for hepatic TAG accumulation in carriers of the I148M allele are the subject of vivid debate. While PNPLA3 has been suggested to act either as a TAG lipase (6, 21) or as a lipogenic LPA acyltransferase (17), the present study employing a cultured human hepatocyte model provides evidence for a more complex mode of PNPLA3 action in hepatocyte TAG remodeling, an activity that is partially inhibited in the I148M variant. The key observations supporting this interpretation are: *i*) PNPLA3^{WT} overexpression causes no significant net reduction of cellular TAGs; *ii*) PNPLA3^{I148M} induces net accumulation of TAGs and slows down TAG hydrolysis upon cellular lipid depletion (6, 15); *iii*) Both PNPLA3^{WT} and PNPLA3^{I148M} induce cellular enrichment of SFA- and MUFA-containing TAGs, and simultaneously enrichment of PCs with PUFAs; *iv*) Upon [¹³C] glycerol labeling, PNPLA3^{WT} is associated with cellular enrichment of newly synthesized [¹³C]TAG species having 52 or 50 acyl carbons and carrying one or several 18:1n-9 FAs, whereas PNPLA3^{I148M} associates with the corresponding unlabeled TAGs; *v*) Upon [D17]18:1n-9 labeling in

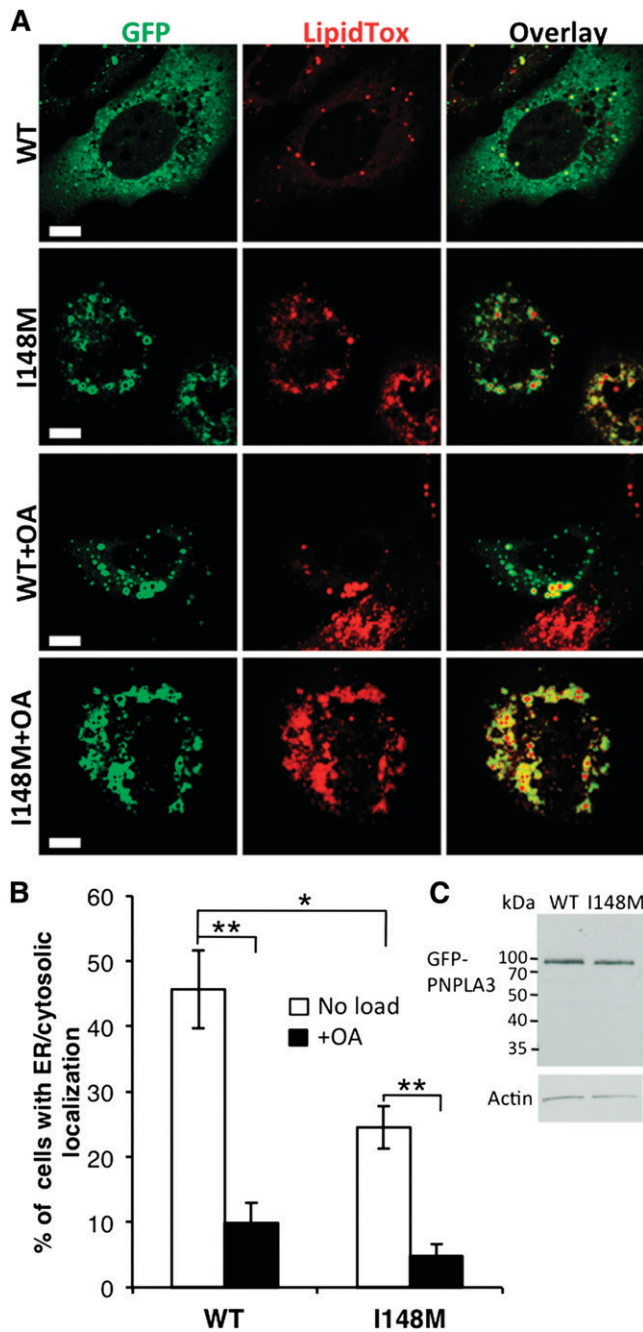


Fig. 4. PNPLA3^{I148M} localizes more extensively to LDs than PNPLA3^{WT}. **A:** HuH7 cells were transfected with GFP-PNPLA3^{WT} (WT) or -PNPLA3^{I148M} (I148M) in the absence (six top panels) or presence (six bottom panels) of 24 h treatment with 200 μ M oleic acid (OA), then fixed and stained with LipidTox to visualize LDs. The images are confocal and represent a single focal plane, Scale bars, 10 μ m. **B:** Quantification of GFP-PNPLA3^{WT} or -PNPLA3^{I148M} distribution in the presence or absence of OA treatment by fluorescence microscopy analysis. The bars represent percentage of cells in the field exhibiting predominantly an ER/cytosolic staining pattern. Data are expressed as mean \pm SEM; number of fields, 10 per treatment; number of cells, 89–127. * P < 0.01, ** P < 0.001. **C:** Western analysis of the cells with anti-GFP, showing that the expressed fusion proteins are intact and present at similar levels.


complete growth medium, PNPLA3^{WT}, but not PNPLA3^{I148M}, enhances the incorporation of this deuterated FA into TAGs during 24 h and speeds up its turnover during longer labeling times. Thus, even though PNPLA3^{WT} does not significantly affect the total cellular TAG content, it has a distinct impact on the incorporation and removal of its preferred substrate fatty acyl moiety, 18:1n-9 (9), into/from TAGs, an activity defective in PNPLA3^{I148M}.

The facts that the PNPLA3-induced alterations in molecular species composition observed in TAGs, DAGs, and PCs were not present in PAs, and that the total cellular PA content was not significantly altered, suggest that PNPLA3 may not significantly modify lipid syntheses at the level of PA (17). However, unaltered PA steady state concentrations do not rule out dynamic changes of PA metabolism. In earlier work with the same hepatic cell model, we found no significant effect of PNPLA3^{WT} or PNPLA3^{I148M} on de novo lipogenesis as measured by [³H]acetate labeling (15).

Acyl chain remodeling is considered a frequent process in hepatocytes, and in addition to acyltransferases, transacylases are present that catalyze the acyl chain transfer (32, 33). Our cell model data employing acute overexpression of PNPLA3 reveals that PNPLA3 has the capacity to modify the TAG, DAG, and PC FA composition. This could involve hydrolysis of TAG FA ester bonds, followed by activation of the released FAs by CoA and transfer to the FA scavenging acceptor lyso-PC to form PC (34) or to DAGs to resynthesize TAGs. Alternatively, PNPLA3 may catalyze or facilitate CoA-independent direct FA transfer between lipids, designated transacylase activity (7). PNPLA3 has been shown to display both TAG lipase and transacylase activities in vitro (6–8). The present data are compatible with TAG remodeling via either of these routes. The observed enrichment of cellular TAGs with SFA- and MUFA-containing species suggests that the PNPLA3-associated remodeling activity exhibits FA selectivity. However, PNPLA3 displays no fatty acyl-CoA DAG acyltransferase activity in vitro, suggesting that PNPLA3 does not directly mediate FA reesterification into TAGs (9). Instead, the transacylation activity assigned for PNPLA3 (7) may target selected FAs. The fact that PNPLA3^{I148M} associated in [¹³C]glycerol labeling experiments with the preexisting unlabeled 52:1 and 50:1 TAGs and the WT protein with the corresponding newly synthesized species, the retardation of TAG hydrolysis by PNPLA3^{I148M}, as well as the lack of effect by PNPLA3^{I148M} on [D17]18:1n-9 labeling of TAGs and turnover of the label, suggested that a hallmark property of the NAFLD-associated PNPLA3^{I148M} is a defect in TAG remodeling. Because each cycle of FA ester hydrolysis and reesterification results in a “leak” of FAs for oxidation, phospholipid synthesis, or VLDL assembly (32), such a defect may eventually result in net TAG accumulation. In chronic long-term accumulation of large LDs rich in hydrophobic TAG species, the mobilization rate of TAG is further decelerated (35). Thus, altered TAG remodeling in cells expressing PNPLA3^{I148M} may generate LDs with a TAG composition resistant to hydrolysis. This interpretation is compatible with the complex phenotypic effects of human PNPLA3^{I148M} expressed in the liver of transgenic mice (22) and the published human data (21).

PNPLA3 was recently shown to localize to LDs in both hepatocytes (6) and fibroblast-like cells (23). Our morphologic observations in hepatic cells suggest that PNPLA3^{I148M} associates more extensively with LD surfaces than PNPLA3^{WT}. Moreover, FA loading of the hepatoma cells enhanced the association of both PNPLA3^{WT} and PNPLA3^{I148M} with the enlarged LDs. While the effect of PNPLA3^{I148M} on hepatocyte LD size has been established (6, 22, 23), its increased association with LDs is a novel observation. It is possible that upon FA loading, the increase in LD size, and in the amount of stored TAG are sufficient to enhance PNPLA3 association with the LDs, and that this effect is more pronounced with PNPLA3^{I148M} which facilitates net TAG accumulation. On the other hand, the more extensive LD localization of PNPLA3^{I148M} may reflect its altered function in TAG metabolism. It could, for instance, modify the recruitment of cofactors regulating lipase or FA reesterification activity on the LD surface (23).

PNPLA3 transcription is, similarly to a number of lipogenic genes, induced by refeeding glucose and insulin (10–12), consistent with the notion that its function is not predominantly lipolytic. If PNPLA3 acts to control cycles of TAG remodeling, what would be the physiologic role of this activity? We find it possible that, under conditions of insulin-induced lipogenesis, increased levels of PNPLA3 are needed to maintain the dynamic metabolic properties of the rapidly growing LDs and selective sorting of FAs between the pools of storage and membrane lipids.

As a conclusion, our data suggests that PNPLA3 facilitates hepatic TAG remodeling in a FA-selective manner. The present findings are consistent with a model in which PNPLA3^{I148M} induces a defect in TAG remodeling, resulting in hepatocellular TAG accumulation. 

The authors are grateful to Liisa Arala, Eeva Jääskeläinen, Anne Salo, and Mia Urjansson for skilled technical assistance.

REFERENCES

- Cohen, J. C., J. D. Horton, and H. H. Hobbs. 2011. Human fatty liver disease: old questions and new insights. *Science*. **332**: 1519–1523.
- Younossi, Z. M., M. Stepanova, M. Afendy, Y. Fang, Y. Younossi, H. Mir, and M. Srishord. 2011. Changes in the prevalence of the most common causes of chronic liver diseases in the United States from 1988 to 2008. *Clin. Gastroenterol. Hepatol.* **9**: 524–530.
- Kotronen, A., J. Westerbacka, R. Bergholm, K. H. Pietiläinen, and H. Yki-Järvinen. 2007. Liver fat in the metabolic syndrome. *J. Clin. Endocrinol. Metab.* **92**: 3490–3497.
- Romeo, S., J. Kozlitina, C. Xing, A. Pertsemlidis, D. Cox, L. A. Pennacchio, E. Boerwinkle, J. C. Cohen, and H. H. Hobbs. 2008. Genetic variation in PNPLA3 confers susceptibility to nonalcoholic fatty liver disease. *Nat. Genet.* **40**: 1461–1465.
- Sookoian, S., and C. J. Pirola. 2011. Meta-analysis of the influence of I148M variant of patatin-like phospholipase domain containing 3 gene (PNPLA3) on the susceptibility and histological severity of nonalcoholic fatty liver disease. *Hepatology*. **53**: 1883–1894.
- He, S., C. McPhaul, J. Z. Li, R. Garuti, L. Kinch, N. V. Grishin, J. C. Cohen, and H. H. Hobbs. 2010. A sequence variation (I148M) in PNPLA3 associated with nonalcoholic fatty liver disease disrupts triglyceride hydrolysis. *J. Biol. Chem.* **285**: 6706–6715.
- Jenkins, C. M., D. J. Mancuso, W. Yan, H. F. Sims, B. Gibson, and R. W. Gross. 2004. Identification, cloning, expression, and purification of three novel human calcium-independent phospholipase A2 family members possessing triacylglycerol lipase and acylglycerol transacylase activities. *J. Biol. Chem.* **279**: 48968–48975.
- Lake, A. C., Y. Sun, J. L. Li, J. E. Kim, J. W. Johnson, D. Li, T. Revett, H. H. Shih, W. Liu, J. E. Paulsen, et al. 2005. Expression, regulation, and triglyceride hydrolase activity of Adiponutrin family members. *J. Lipid Res.* **46**: 2477–2487.
- Huang, Y., J. C. Cohen, and H. H. Hobbs. 2011. Expression and characterization of a PNPLA3 protein isoform (I148M) associated with nonalcoholic fatty liver disease. *J. Biol. Chem.* **286**: 37085–37093.
- Moldes, M., G. Beauregard, M. Faraj, N. Peretti, P. H. Duchezau, M. Laville, R. Rabasa-Lhoret, H. Vidal, and K. Clement. 2006. Adiponutrin gene is regulated by insulin and glucose in human adipose tissue. *Eur. J. Endocrinol.* **155**: 461–468.
- Rae-Whitcombe, S. M., D. Kennedy, M. Voyles, and M. P. Thompson. 2010. Regulation of the promoter region of the human adiponutrin/PNPLA3 gene by glucose and insulin. *Biochem. Biophys. Res. Commun.* **402**: 767–772.
- Soronen, J., P. P. Laurila, J. Naukkarinen, I. Surakka, S. Ripatti, M. Jauhainen, V. M. Olkkonen, and H. Yki-Järvinen. 2012. Adipose tissue gene expression analysis reveals changes in inflammatory, mitochondrial respiratory and lipid metabolic pathways in obese insulin-resistant subjects. *BMC Med. Genomics*. **5**: 9.
- Huang, Y., S. He, J. Z. Li, Y. K. Seo, T. F. Osborne, J. C. Cohen, and H. H. Hobbs. 2010. A feed-forward loop amplifies nutritional regulation of PNPLA3. *Proc. Natl. Acad. Sci. USA*. **107**: 7892–7897.
- Dubuquoy, C., C. Robichon, F. Lasnier, C. Langlois, I. Dugail, F. Foufelle, J. Girard, A. F. Burnol, C. Postic, and M. Moldes. 2011. Distinct regulation of adiponutrin/PNPLA3 gene expression by the transcription factors ChREBP and SREBP1c in mouse and human hepatocytes. *J. Hepatol.* **55**: 145–153.
- Perttilä, J., C. Huaman-Samanez, S. Caron, K. Tanhuanpää, B. Staels, H. Yki-Järvinen, and V. M. Olkkonen. 2012. PNPLA3 is regulated by glucose in human hepatocytes, and its I148M mutant slows down triglyceride hydrolysis. *Am. J. Physiol. Endocrinol. Metab.* **302**: E1063–E1069.
- Qiao, A., J. Liang, Y. Ke, C. Li, Y. Cui, L. Shen, H. Zhang, A. Cui, X. Liu, C. Liu, et al. 2011. Mouse patatin-like phospholipase domain-containing 3 influences systemic lipid and glucose homeostasis. *Hepatology*. **54**: 509–521.
- Kumari, M., G. Schoiswohl, C. Chitraju, M. Paar, I. Cornaciu, A. Y. Rangrez, N. Wongsiriroj, H. M. Nagy, P. T. Ivanova, S. A. Scott, et al. 2012. Adiponutrin functions as a nutritionally regulated lysophosphatidic acid acyltransferase. *Cell Metab.* **15**: 691–702.
- Basantani, M. K., M. T. Sitnick, L. Cai, D. S. Brenner, N. P. Gardner, J. Z. Li, G. Schoiswohl, K. Yang, M. Kumari, R. W. Gross, et al. 2011. Pnpla3/Adiponutrin deficiency in mice does not contribute to fatty liver disease or metabolic syndrome. *J. Lipid Res.* **52**: 318–329.
- Chen, W., B. Chang, L. Li, and L. Chan. 2010. Patatin-like phospholipase domain-containing 3/adiponutrin deficiency in mice is not associated with fatty liver disease. *Hepatology*. **52**: 1134–1142.
- Kumashiro, N., T. Yoshimura, J. L. Cantley, S. K. Majumdar, F. Guebre-Egziabher, R. Kursawe, D. F. Vatner, I. Fat, M. Kahn, D. M. Erion, et al. 2013. Role of patatin-like phospholipase domain-containing 3 on lipid-induced hepatic steatosis and insulin resistance in rats. *Hepatology*. **57**: 1763–1772.
- Pirazzi, C., M. Adiels, M. A. Burza, R. M. Mancina, M. Levin, M. Stahlman, M. R. Taskinen, M. Orho-Melander, J. Perman, A. Pujia, et al. 2012. Patatin-like phospholipase domain-containing 3 (PNPLA3) I148M (rs738409) affects hepatic VLDL secretion in humans and in vitro. *J. Hepatol.* **57**: 1276–1282.
- Li, J. Z., Y. Huang, R. Karaman, P. T. Ivanova, H. A. Brown, T. Roddy, J. Castro-Perez, J. C. Cohen, and H. H. Hobbs. 2012. Chronic overexpression of PNPLA3I148M in mouse liver causes hepatic steatosis. *J. Clin. Invest.* **122**: 4130–4144.
- Chamoun, Z., F. Vacca, R. G. Parton, and J. Gruenberg. 2013. PNPLA3/adiponutrin functions in lipid droplet formation. *Biol. Cell*. **105**: 219–233.
- Nakabayashi, H., K. Taketa, K. Miyano, T. Yamane, and J. Sato. 1982. Growth of human hepatoma cells lines with differentiated functions in chemically defined medium. *Cancer Res.* **42**: 3858–3863.
- Folch, J., M. Lees, and G. H. Sloane Stanley. 1957. A simple method for the isolation and purification of total lipides from animal tissues. *J. Biol. Chem.* **226**: 497–509.
- Käkelä, R., P. Somerharju, and J. Tyynelä. 2003. Analysis of phospholipid molecular species in brains from patients with infantile and juvenile neuronal-ceroid lipofuscinosis using liquid chromatography-electrospray ionization mass spectrometry. *J. Neurochem.* **84**: 1051–1065.

27. Haimi, P., A. Uphoff, M. Hermansson, and P. Somerharju. 2006. Software tools for analysis of mass spectrometric lipidome data. *Anal. Chem.* **78**: 8324–8331.
28. Käkälä, R., A. Käkälä, S. Kahle, P. H. Becker, A. Kelly, and R. Furness. 2005. Fatty acid signatures in plasma of captive herring gulls as indicators of demersal or pelagic fish diet. *Mar. Ecol. Prog. Ser.* **293**: 191–200.
29. Bligh, E. G., and W. J. Dyer. 1959. A rapid method of total lipid extraction and purification. *Can. J. Biochem. Physiol.* **37**: 911–917.
30. Hölttä-Vuori, M., V. T. Salo, Y. Ohsaki, M. L. Suster, and E. Ikonen. 2013. Alleviation of seipinopathy-related ER stress by triglyceride storage. *Hum. Mol. Genet.* **22**: 1157–1166.
31. Wold, S., and M. Sjöström. 1977. SIMCA: a method for analyzing chemical data in terms of similarity and analogy. In *Chemometrics: Theory and Application*. B. Kowalski, editor. American Chemical Society, Washington, DC. 243–282.
32. Lankester, D. L., A. M. Brown, and V. A. Zammit. 1998. Use of cytosolic triacylglycerol hydrolysis products and of exogenous fatty acid for the synthesis of triacylglycerol secreted by cultured rat hepatocytes. *J. Lipid Res.* **39**: 1889–1895.
33. Yamashita, A., Y. Hayashi, Y. Nemoto-Sasaki, M. Ito, S. Oka, T. Tanikawa, K. Waku, and T. Sugiura. 2014. Acyltransferases and transacylases that determine the fatty acid composition of glycerolipids and the metabolism of bioactive lipid mediators in mammalian cells and model organisms. *Prog. Lipid Res.* **53**: 18–81.
34. Pérez-Chacón, G., A. M. Astudillo, D. Balgoma, M. A. Balboa, and J. Balsinde. 2009. Control of free arachidonic acid levels by phospholipases A2 and lysophospholipid acyltransferases. *Biochim. Biophys. Acta.* **1791**: 1103–1113.
35. Raclot, T. 2003. Selective mobilization of fatty acids from adipose tissue triacylglycerols. *Prog. Lipid Res.* **42**: 257–288.